The Astrophysical Journal Letters, 807:L32 (5pp), 2015 July 10 doi:10.1088/2041-8205/807/2/L32

VOLATILE DEPLETION IN THE TW HYDRAE DISK ATMOSPHERE

Fujun Du[1], Edwin A. Bergin[1], and Michiel R. Hogerheijde[2]
[1] Department of Astronomy, University of Michigan, 311 West Hall, 1085 S. University Avenue, Ann Arbor, MI 48109, USA; fdu@umich.edu
[2] Leiden Observatory, Leiden University, Post Office Box 9513, 2300 RA Leiden, Netherlands
Received 2015 May 12; accepted 2015 June 10; published 2015 July 13

ABSTRACT

An abundance decrease in carbon- and oxygen-bearing species relative to dust has been frequently found in planet-forming disks, which can be attributed to an overall reduction of gas mass. However, in the case of TW Hya, the only disk with gas mass measured directly with HD rotational lines, the inferred gas mass ($\lesssim$0.005 solar mass) is significantly below the directly measured value ($\gtrsim$0.05 solar mass). We show that this apparent conflict can be resolved if the elemental abundances of carbon and oxygen are reduced in the upper layers of the outer disk but are normal elsewhere (except for a possible enhancement of their abundances in the inner disk). The implication is that in the outer disk, the main reservoir of the volatiles (CO, water, …) resides close to the midplane, locked up inside solid bodies that are too heavy to be transported back to the atmosphere by turbulence. An enhancement in the carbon and oxygen abundances in the inner disk can be caused by inward migration of these solid bodies. This is consistent with estimates based on previous models of dust grain dynamics. Indirect measurements of the disk gas mass and disk structure from species such as CO will thus be intertwined with the evolution of dust grains, and possibly also with the formation of planetesimals.

Key words: astrochemistry – circumstellar matter – molecular processes – planetary systems – planet–disk interactions – planets and satellites: atmospheres

1. INTRODUCTION

Observations and modeling of transitional disks have pointed to an apparent lack of gas relative to their dust content, particularly at larger distances from the star. Early observations (see, e.g., Skrutskie et al. 1991 and Yamashita et al. 1993) show that the CO emission are much lower than expected from dust emission and molecular cloud composition. A recent *Herschel*/PACS survey finds that transitional disks have weaker O I 63 μm emission than their full disk counterparts, even if they have a similar continuum at 63 μm (Howard et al. 2013; Keane et al. 2014). One interpretation of this is that the gas mass is reduced, or, equivalently in effect, that the transitional disks are less flared than their full disk counterpart (Keane et al. 2014). Aresu et al. (2014) find that with a normal gas-to-dust ratio, models of the O I 63 μm emission for disks in Taurus tend to over-predict the line intensity. Similarly, detailed modeling of the prototypical transitional disk, TW Hya, suggest a small gas mass $(0.5\text{–}5)\times10^{-3}$ $M_\odot$ (and small gas-to-dust mass ratio; Thi et al. 2010; Kamp et al. 2013; Williams & Best 2014).

However, the gas mass in these studies is only inferred rather than directly measured. The main constituent of the gas is hydrogen, mostly in molecular form, followed by helium, both of which defy direct detection in the bulk of the disk, because their line excitation requires high temperature. So the gas mass is inferred from other agents, such as the commonly used CO lines or dust continuum, in combination with radiative transfer and thermo-chemical models. Fortunately, with *Herschel*, it is possible to measure the gas mass in a much more direct way, by observing the rotational transition lines of HD, an isotopologue of molecular hydrogen. The translation of HD intensity to H_2 mass is more straightforward because there is no complex chemistry involved (though the result depends on the temperature structure). Direct measurement of the gas mass of TW Hya based on *Herschel* observation of HD lines gives mass $\gtrsim$0.05 $M_\odot$ (Bergin et al. 2013), much higher than the values in some of the previous studies.

To reconcile the two classes of seemingly disparate results on the gas mass of TW Hya, here we show that it is *not* the overall gas mass—the mass of atomic and molecular hydrogen—that is reduced, but rather it is the mass of the ice-forming species, such as CO and H_2O, reduced in the upper layers of the outer disk. It is these upper layers that are emissive and detectable by astronomical observations. The depletion of CO relative to hydrogen in DM Tau and GG Tau has been found by Dutrey et al. (1997) based on excitation arguments, and in TW Hya by Favre et al. (2013) based on direct comparison of the CO isotopologue emission with the HD result. Reduction of the water content has been suggested by Bergin et al. (2010) and Hogerheijde et al. (2011, supporting material). Since CO and H_2O are the main bearers of carbon and oxygen in the upper layers (below the photodissociated layer), the total abundances of elemental carbon and oxygen are lowered. This affects other species chemically linked to them. We also establish that this effect is evident only in the outer disk (beyond the water and CO snow line), while in the inner disk the opposite—namely enhancement of the oxygen and carbon abundances—might be taking place. A possible physical mechanism based on dust grain settling and migration is provided at the end.

2. MODELS

We run two models for TW Hya using a thermo-chemical and radiative-transfer code (Du & Bergin 2014). The system is evolved for 1 Myr. Both models assume a disk with total gas mass 0.05 $M_\odot$ as constrained by the HD rotational lines (Bergin et al. 2013), a distance of 51 pc (Mamajek 2005), and an inclination angle of 7° (Qi et al. 2004). The dust mass is not very well constrained, so we use a uniform gas-to-dust mass ratio of 100 for both models. We assume three components for the disk structure: an optically thin component inside ~3.5 AU,

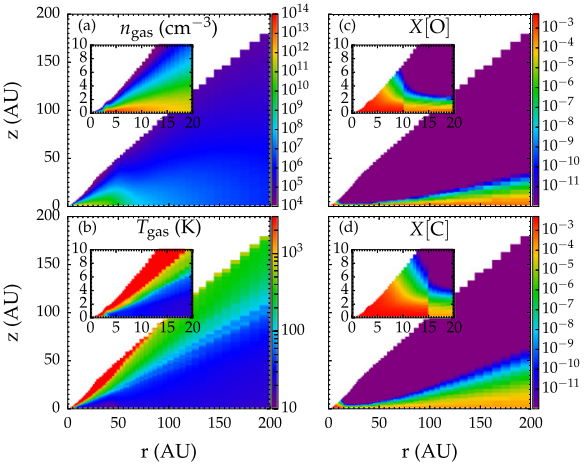

Figure 1. Distribution of disk physical parameters used in the models. (a): Gas density distribution in the two models. (b): Gas temperature distribution inthe model in which the oxygen and carbon abundances are changed; for the model with full oxygen and carbon abundances, the gas temperature distribution is slightly different due to changes in the heating and cooling rates of oxygen- and carbon-bearing species. (c) and (d): Distribution of oxygen and carbon abundances relative to hydrogen nuclei in the model in which their abundances are changed.

a component tapering at ∼50 AU (Andrews et al. 2012; Menu et al. 2014), and a component extended to ∼200 AU. The mass ratio of the three components is 10^{-4}:20:1. The outer two components have a surface density profile $\Sigma \propto r^{-3/2}$. The disk 3D density and temperature structure are determined based on vertical hydrostatic equilibrium, calculated through iterative Monte Carlo simulation of dust radiative transfer, which also yields a spectral energy distribution that matches observation. The resulting 870 μm continuum map of TW Hya resembles the observed one of Andrews et al. (2012), though we spend no effort to match the visibility profile. The distribution of gas density and temperature is shown in panels (a) and (b) of Figure 1. The only difference between the two models lies in the abundances of oxygen and carbon (relative to hydrogen). The first model has canonical "low-metal" interstellar medium (ISM) oxygen and carbon abundances (Garrod et al. 2008) in the whole disk, while the second model has reduced oxygen and carbon abundances in the upper layers of the outer disk, and enhanced oxygen and carbon abundances in the inner disk (see panels (c) and (d) of Figure 1). The degree of reduction for oxygen and carbon are based on an analytical prescription, the exact form of which is manually adjusted for a best fit. Carbon is less reduced than oxygen in the outer disk, inspired by the difference in the evaporation temperatures (Öberg et al. 2011) of water and the major bearers of carbon (CO and CO_2). The enhancement in the inner disk is simply implemented with a step function. This empirical approach is particularly tailored to match the observational data. Future self-consistent study is needed.

3. RESULTS

The code predict intensities for a suite of transitions of different species, including C II, O I, H_2O, HD, and the CO isotopologues, which have been detected by observation. The resulting line intensities from the two models are compared with the observed values in Figure 2 (for the numerical values see Table 1). In agreement with previous studies (Thi et al. 2010; Kamp et al. 2013; Keane et al. 2014; Williams & Best 2014), the model without elemental depletion consistently over-predicts the line intensities of CO, water, and a few other species for TW Hya, while the model with depleted oxygen and carbon abundances matches the observational data. There are a few lines that most clearly require oxygen and carbon to be depleted in the atmosphere of the outer disk, including the O I 63 μm, the CO and $C^{18}O$ low-J lines, and all the water ground state lines.

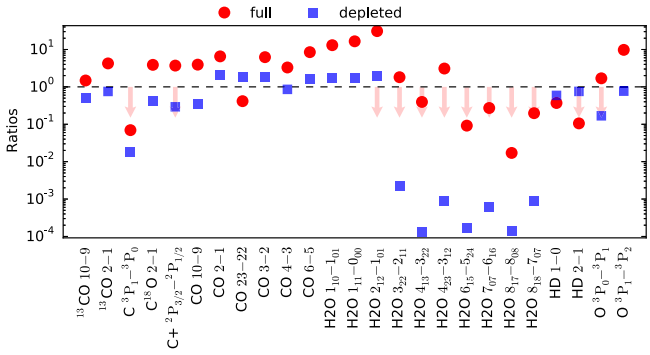

Figure 2. Ratios between the modeled and observed intensities for a selection of lines. Red dot: with full oxygen and carbon abundances; blue rectangle: with depleted oxygen and carbon abundances. The arrows mean that the observed values are upper limits. The relative measurement error of the observational data is usually much less than 50%. For the detected lines, a perfect fit would land on the dashed line.

In both models, the water $1_{10} - 1_{01}$, $1_{11} - 0_{00}$, and $2_{12} - 1_{01}$ lines originate from $\gtrsim$20 AU, well beyond the water snow line. Gas phase water molecules in this region are mainly produced through photodesorption of water ice (Bergin et al. 2010; Hogerheijde et al. 2011; Kamp et al. 2013), with their rates established by experiment (Öberg et al. 2009). A normal oxygen abundance in the outer disk over-predicts their intensities by more than one order of magnitude. The situation is similar for the CO and $C^{18}O$ low-J lines (see also Favre et al. 2013). The O I and C II lines mainly originate from near the water snow line at $r \lesssim 4$ AU in the model with reduced oxygen and carbon abundances, coincident with where the water infrared lines originate (Zhang et al. 2013). With normal oxygen and carbon abundances, additional contribution to the emission arises in gas out to 10–20 AU, which make them too strong, by a factor of 5 in the case of O I. We note that a deficit of elemental carbon in the disk atmosphere has been suggested for the Herbig Be star HD 100546 by Bruderer et al. (2012).

In the model with elemental depletion, we let the carbon and oxygen abundances gradually return to normal when approaching the CO snow line (∼20 AU) from outside. This is required to account for the observed high-J and rovibrational CO lines, as well as O I and the numerous mid-infrared transitions of water vapor (see Figure 3). This scenario resonates with the recent result on the CO/H_2 ratio, which is $\sim 1.6 \times 10^{-4}$ very close to the star in RW Aurigae A (France et al. 2014). For the ^{13}CO 10–9 and CO 10–9 and 23–22 transitions, canonical carbon and oxygen abundances in the inner disk of the depleted model are not enough to reproduce the data; these three lines are under-predicted by about one order of magnitude. Along our line of reasoning, one intriguing possibility is that the carbon and oxygen abundances are enhanced (van Dishoeck et al. 2014), rather than reduced, in the inner disk. In fact, if we increase the abundance of carbon and oxygen by a factor of 10 over the ISM value within ∼15 AU (see the insets in panels (c) and (d) of Figure 1), the CO 10–9 and 23–22 and the ^{13}CO

Table 1
Comparison Between Modeled and Observed Integrated Line Fluxes

Molecule	Line	λ (μm)	E_{up} (K)	Observed	Full	Depleted	Reference
				(10^{-18} W m^{-2})			
C^+	$^2P_{3/2}$–$^2P_{1/2}$	157.74	91	<6.6	24.4	1.9	5
C	$^3P_1$–$^3P_0$	609.14	24	<0.4	0.03	0.01	7
O	$^3P_1$ –^{3} P_2	63.18	228	36.5 ± 12.1	356	31.3	5
	$^3P_0$–$^3P_1$	145.53	327	<5.5	9.3	1.1	5
CO	2–1	1300.41	17	0.04	0.26	0.08	4
	3–2	866.96	33	0.14	0.87	0.25	4
	4–3	650.25	55	0.59	1.95	0.50	7
	6–5	433.55	116	0.61	5.17	0.98	4
	10–9	260.24	304	2.13	8.37	1.01	3
	23–22	113.46	1524	4.4	1.82	8.22	3
^{13}CO	2–1	1300.41	17	0.02	0.08	0.02	2
^{13}CO	10–9	260.24	304	0.36	0.53	0.19	3
C ^{18}O	2–1	1300.41	17	0.006	0.02	0.003	2
H_2O	···	21–35	800–3000		See Figure 3		6
OH	···	21–35	400–4000				6
H_2O	$8_{18} - 7_{07}$	63.32	1071	<12.3	2.4	0.03	6
	$7_{07} - 6_{16}$	71.95	844	<12.7	3.5	0.02	6
	$8_{17} - 8_{08}$	72.03	1270	<3.5	0.06	0.008	6
	$4_{23} - 3_{12}$	78.74	432	<3.9	12.1	0.01	6
	$6_{15} - 5_{24}$	78.93	781	<5.4	0.5	0.003	6
	$3_{22} - 2_{11}$	89.99	297	<6.1	11.0	0.02	6
	$4_{13} - 3_{22}$	144.52	396	<0.6	0.2	0	6
	$2_{12} - 1_{01}$	179.53	114	<0.9	27.9	1.80	6
	$1_{10} - 1_{01}$	538.29	61	0.17 ± 0.01	2.2	0.28	3
	$1_{11} - 0_{00}$	269.27	53	0.61 ± 0.04	10.1	1.03	3
HD	1–0	112.07	128	6.3 ± 0.7	2.3	4.0	1
	2–1	56.23	384	<8	0.8	6.0	1

Note. The "Full" column is for the model with canonical carbon and oxygen abundances, and the "Depleted" column is for the model with reduced carbon and oxygen abundances.

References. 1. Bergin et al. (2013), 2. Favre et al. (2013), 3. Hogerheijde et al. (2011), 4. Qi et al. (2006), synthesized beam corresponding to 100 AU, 5. Thi et al. (2010), 6. Zhang et al. (2013), 7. Tsukagoshi et al. (2015).

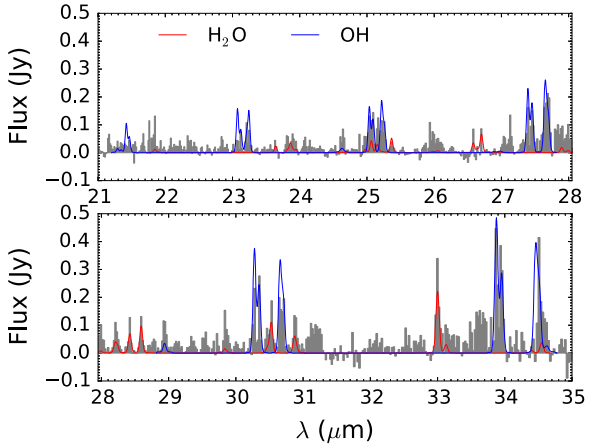

Figure 3. Fitting to the *Spitzer/IRS* H_2O and OH lines. The *Spitzer* spectrum (in gray) is from Zhang et al. (2013).

10–9 lines would be in good agreement with observations, as shown in Figure 2, while still keeping other lines consistent with observations. Inward migration and evaporation of icy bodies is predicted to cause such an enhancement of CO and water vapor in the inner disk (Cuzzi & Zahnle 2004; Ciesla & Cuzzi 2006).

In the above we have assumed that only oxygen and carbon are differentially depleted in the outer disk atmosphere, and have left nitrogen intact. This is a reasonable assumption, considering that solar system ices as traced by comets are well known to be nitrogen-poor (Wyckoff et al. 1991). One interesting outcome of this assumption is that by depleting oxygen (and carbon, but to a lower degree) over nearly the entire disk the gas will become rich in carbon (particularly inside the CO snow line) and nitrogen-bearing molecules. As an example, Figure 4 shows that the column densities of species containing C–N, C–H, and N–H bonds can be increased by up to two orders of magnitude in the depleted model. This is in line with the recent results on the enhanced abundances of C_2H and CN in evolved protoplanetary disks (Kastner et al. 2014).

Depletion of carbon and oxygen in the outer disk also affects the HD emission. This is because the cooling efficiency due to species bearing these two elements are changed, so that the temperature in the outer disk becomes higher, leading to a stronger HD emission. For example, 80% of the HD 112 μm emission comes from within 80 AU in the model with no depletion, while with depletion 60% arises within the same radius (i.e., the outer disk contributes more). Though, as pointed out by Röllig et al. (2007), the energy balance

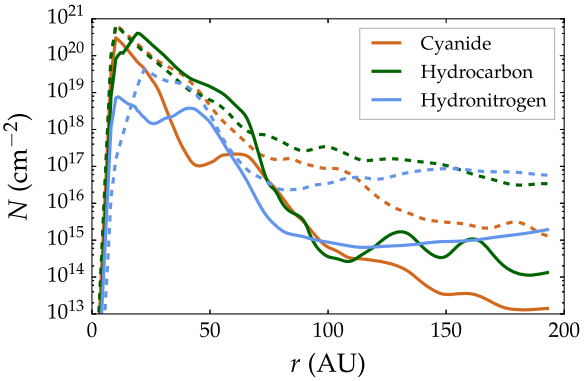

Figure 4. Comparison between the column density of non-oxygen-bearing cyanide (containing C–N bonds), hydrocarbon (containing C–H bonds), and hydronitrogen (containing N–H bonds) from two models with full (solid lines) and reduced (dashed lines) oxygen and carbon abundances.

calculation could be subject to considerable uncertainty in the tenuous regions.

4. DISCUSSIONS

The depletion of oxygen and carbon relative to hydrogen solves the puzzle regarding the gas mass of the TW Hya disk. The only known gas-loss mechanism that preferentially removes species containing oxygen and/or carbon (mainly H_2O and CO) rather than atomic or molecular hydrogen is ice mantle formation on dust grains. We emphasize that ice mantle formation and grain surface chemical reactions by themselves do not reduce the local elemental abundances (gas + ice) in the atmosphere. Reboussin et al. (2015) find that CO can be transformed into other species such as CO_2 and CH_4 on the dust grain surfaces (see also Bergin et al. 2014). However, what we find is that if the ice-coated grains stay in the upper atmosphere, desorption and dissociation by UV photons will release H_2O, O, OH, CO, etc. to the gas phase, and the emission from them will be much stronger than observations. The key point is that the dust grains also grow through coagulation, and as they grow, they settle to the disk midplane (Dullemond & Dominik 2005; Akimkin et al. 2013), where they continue to grow bigger and get assembled into planetesimals that may eventually grow to tens of kilometers in size (Stepinski & Valageas 1997), possibly accompanied by inward drift (Laibe et al. 2012). The majority of the oxygen and carbon originally frozen onto the dust grains in the atmosphere thus ends up inside solid bodies in the midplane of the disk (Bergin et al. 2010; Hogerheijde et al. 2011; Najita et al. 2013).

A reverse process to dust settling described above must also be considered. Dust grains in the upper layers can be replenished (Kelling & Wurm 2011) by the midplane reservoir through turbulent diffusion. TW Hya has relatively weak turbulence (Hughes et al. 2011), which yields a ratio between the scale heights of dust grains and gas of the order of 0.1 (Cuzzi & Weidenschilling 2006; Brauer et al. 2008). This is consistent with the scale height of oxygen and carbon elements found in the present work.

Birnstiel & Andrews (2014) find that the inward migration of dust grains combined with gas drag produces a sharp edge in the dust distribution. What we add to this picture is that the inward migration (together with growth and vertical settling) of dust grains also removes species such as CO and H_2O from the outer disk atmosphere, though emission of the leftover of these species that remain in the outer region can still be significant.

The dust grains will eventually fall into the central star (may get disintegrated on its way to the star), or become part of a planetesimal, depending on whether they can overcome the fragmentation barrier (Johansen et al. 2008; Birnstiel et al. 2010) to grow large, and whether they can pass the radial drift barrier to avoid falling into the star. It is a theoretical challenge to bypass the two barriers to maintain enough dust material in the disk to form planets. Empirically, there is evidence for the early presence of large planetesimals for our solar system from cosmochemical record of rocks. It is known that parental bodies ($\gtrsim$50 km) of meteorites had already begun to form within a million years of the condensation of calcium–aluminum-rich inclusions (CAIs; Kleine et al. 2005; Qin et al. 2008; Kruijer et al. 2014), and CAIs are generally considered the oldest bodies of the solar system (Amelin et al. 2002). If systems such as TW Hya are similar to the solar system, then their planetesimals formed at an early stage will be rich in carbon- and oxygen-bearing ices.

F.D. and E.A.B. are supported by grant NNX12A193G from the NASA Origin of Solar Systems Program. We thank Ilse Cleeves and Fred Ciesla for discussions.

REFERENCES

Akimkin, V., Zhukovska, S., Wiebe, D., et al. 2013, ApJ, 766, 8
Amelin, Y., Krot, A. N., Hutcheon, I. D., & Ulyanov, A. A. 2002, Sci, 1678, 297
Andrews, S. M., Wilner, D. J., Hughes, A. M., et al. 2012, ApJ, 744, 162
Aresu, G., Kamp, I., Meijerink, R., et al. 2014, A&A, 566, A14
Bergin, E. A., Cleeves, L. I., Gorti, U., et al. 2013, Natur, 493, 644
Bergin, E. A., Hogerheijde, M. R., Brinch, C., et al. 2010, A&A, 521, L33
Bergin, E., Cleeves, L. I., Crockett, N., & Blake, G. 2014, FaDi, 168, 61
Birnstiel, T., & Andrews, S. M. 2014, ApJ, 780, 153
Birnstiel, T., Dullemond, C. P., & Brauer, F. 2010, A&A, 513, A79
Brauer, F., Dullemond, C. P., & Henning, T. 2008, A&A, 480, 859
Bruderer, S., van Dishoeck, E. F., Doty, S. D., & Herczeg, G. J. 2012, A&A, 541, A91
Ciesla, F. J., & Cuzzi, J. N. 2006, Icar, 181, 178
Cuzzi, J. N., & Weidenschilling, S. J. 2006, in Particle-Gas Dynamics and Primary Accretion, ed. D. S. Lauretta & H. Y. McSween (Tucson, AZ: Univ. Arizona Press), 353
Cuzzi, J. N., & Zahnle, K. J. 2004, ApJ, 614, 490
Du, F., & Bergin, E. A. 2014, ApJ, 792, 2
Dullemond, C. P., & Dominik, C. 2005, A&A, 434, 971
Dutrey, A., Guilloteau, S., & Guelin, M. 1997, A&A, 317, L55
Favre, C., Cleeves, L. I., Bergin, E. A., Qi, C., & Blake, G. A. 2013, ApJL, 776, L38
France, K., Herczeg, G. J., McJunkin, M., & Penton, S. V. 2014, arXiv:1409.0861
Garrod, R. T., Weaver, S. L. W., & Herbst, E. 2008, ApJ, 682, 283
Hogerheijde, M. R., Bergin, E. A., Brinch, C., et al. 2011, Sci, 334, 338
Howard, C. D., Sandell, G., Vacca, W. D., et al. 2013, ApJ, 776, 21
Hughes, A. M., Wilner, D. J., Andrews, S. M., Qi, C., & Hogerheijde, M. R. 2011, ApJ, 727, 85
Johansen, A., Brauer, F., Dullemond, C., Klahr, H., & Henning, T. 2008, A&A, 486, 597
Kamp, I., Thi, W.-F., Meeus, G., et al. 2013, A&A, 559, A24
Kastner, J. H., Hily-Blant, P., Rodriguez, D. R., Punzi, K., & Forveille, T. 2014, ApJ, 793, 55
Keane, J. T., Pascucci, I., Espaillat, C., et al. 2014, ApJ, 787, 153
Kelling, T., & Wurm, G. 2011, ApJ, 733, 120
Kleine, T., Mezger, K., Palme, H., Scherer, E., & Münker, C. 2005, GeCoA, 69, 5805
Kruijer, T. S., Touboul, M., Fischer-Gödde, M., et al. 2014, Sci, 344, 1150
Laibe, G., Gonzalez, J.-F., & Maddison, S. T. 2012, A&A, 537, A61
Mamajek, E. E. 2005, ApJ, 634, 1385
Menu, J., van Boekel, R., Henning, T., et al. 2014, A&A, 564, A93
Najita, J. R., Carr, J. S., Pontoppidan, K. M., et al. 2013, ApJ, 766, 134

Öberg, K. I., Linnartz, H., Visser, R., & van Dishoeck, E. F. 2009, ApJ, 693, 1209
Öberg, K. I., Murray-Clay, R., & Bergin, E. A. 2011, ApJL, 743, L16
Qi, C., Ho, P. T. P., Wilner, D. J., et al. 2004, ApJL, 616, L11
Qi, C., Wilner, D. J., Calvet, N., et al. 2006, ApJL, 636, L157
Qin, L., Dauphas, N., Wadhwa, M., Masarik, J., & Janney, P. E. 2008, E&PSL, 273, 94
Reboussin, L., Wakelam, V., Guilloteau, S., Hersant, F., & Dutrey, A. 2015, arXiv:1505.01309
Röllig, M., Abel, N. P., Bell, T., et al. 2007, A&A, 467, 187
Skrutskie, M. F., Snell, R., Dutkevitch, D., et al. 1991, AJ, 102, 1749
Stepinski, T. F., & Valageas, P. 1997, A&A, 319, 1007
Thi, W.-F., Mathews, G., Ménard, F., et al. 2010, A&A, 518, L125
Tsukagoshi, T., Momose, M., Saito, M., et al. 2015, ApJL, 802, L7
van Dishoeck, E. F., Bergin, E. A., Lis, D. C., & Lunine, J. I. 2014, arXiv:1401.8103
Williams, J. P., & Best, W. M. J. 2014, ApJ, 788, 59
Wyckoff, S., Tegler, S. C., & Engel, L. 1991, ApJ, 367, 641
Yamashita, T., Handa, T., Omodaka, T., et al. 1993, ApJL, 402, L65
Zhang, K., Pontoppidan, K. M., Salyk, C., & Blake, G. A. 2013, ApJ, 766, 82